Nanoscale

Accepted Manuscript

This is an *Accepted Manuscript*, which has been through the RSC Publishing peer review process and has been accepted for publication.

Accepted Manuscripts are published online shortly after acceptance, which is prior to technical editing, formatting and proof reading. This free service from RSC Publishing allows authors to make their results available to the community, in citable form, before publication of the edited article. This *Accepted Manuscript* will be replaced by the edited and formatted *Advance Article* as soon as this is available.

To cite this manuscript please use its permanent Digital Object Identifier (DOI®), which is identical for all formats of publication.

More information about *Accepted Manuscripts* can be found in the **Information for Authors**.

Please note that technical editing may introduce minor changes to the text and/or graphics contained in the manuscript submitted by the author(s) which may alter content, and that the standard **Terms & Conditions** and the **ethical guidelines** that apply to the journal are still applicable. In no event shall the RSC be held responsible for any errors or omissions in these *Accepted Manuscript* manuscripts or any consequences arising from the use of any information contained in them.

Cite this: DOI: 10.1039/c0xx00000x

www.rsc.org/xxxxxx

ARTICLE TYPE

The Role of Protein Characteristics in the Formation and Fluorescence of Au Nanoclusters

Yaolin Xu, [a] Jennifer Sherwood,[a] Ying Qin,[b] Dorothy Crowley,[a] Marco Bonizzoni,[c] Yuping Bao[a]*

Received (in XXX, XXX) Xth XXXXXXXXX 20XX, Accepted Xth XXXXXXXXX 20XX

DOI: 10.1039/b000000x

Table of Content

The size and composition of the protein templates are critically important to the formation, fluorescence, and stability of Au nanoclusters

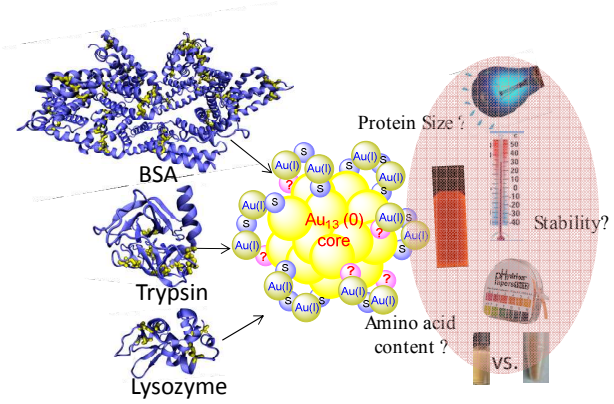

Abstract

Protein-encapsulated gold nanoclusters have shown many advantages over other gold nanocluster systems, including green synthesis, biocompatibility, high water solubility, and the ease of further conjugation. In this article, we systematically investigated the effects of the protein size and amino acid content on the formation and fluorescent properties of gold nanoclusters using four model proteins (bovine serum albumin, lysozyme, trypsin, and pepsin). We discovered that the balance of amine and tyrosine/tryptophan containing residues was critical for the nanocluster formation. Protein templates with low cysteine contents caused blue shifts in the fluorescent emissions and difference in fluorescent lifetimes of the gold nanoclusters. Furthermore, the protein size was found to be a critical factor for the photostability and long-term stability of gold nanoclusters. The size of the protein also affected the Au nanocluster behaviour after immobilization.

Introduction

Fluorescent gold (Au) nanoclusters have attracted much attention due to their emerging photophysical properties and potential applications in biolabeling and sensing.[1-4] Motivated by their potential applications, fluorescent Au nanoclusters have been synthesized using many different capping molecules, such as glutathione,[5] dodecanethiol,[6] dendrimer,[7,8] meso-2,3-dimercapsuccinic acid,[9] Good's buffer,[10,11] DNA,[12-14] and proteins.[15, 16] Among these synthetic methods, protein-directed synthesis is particularly attractive, because proteins serve as environmentally-benign reducing and stabilizing molecules, require only mild reaction conditions, and offer great water solubility and natural biocompatibility.[15] Furthermore, the 3D complexed structures of proteins can withstand a wide range of pH and can be easily conjugated with other systems. So far, a number of proteins have been explored for synthesizing fluorescent Au nanoclusters, including bovine serum albumin (BSA),[16-18] lysozyme,[19, 20] human transferrin,[21, 22] lactoferrin,[23] tryspin,[24] pepsin,[25] insulin,[26] and horseradish peroxidase.[27] Depending upon the reaction conditions, the Au nanoclusters were formed either under protein-denatured conditions[16] or native condition.[26] The protein-templates are expected to influence the nanocluster formation and property because of the diversity in amino acid contents and sequences of proteins.

Most mechanistic studies on the nanocluster formation and fluorescent emissions have been focused on BSA-encapsulated nanoclusters.[17,23] Our previous study showed that the amine-containing amino acids of the proteins were responsible for the Au ion uptake, and the increase of pH to 7 led to the reduction of Au (III) to Au(I); and then tyrosine or tryptophan reduced Au(I) to metallic Au at higher pH (> 10). [28] The fluorescent emission of BSA-Au nanoclusters was proposed to originate from Au_{25} nanoclusters, which were composed of a Au_{13} core and 12 Au(I) sulphur complex, forming six −S−Au(I)−S−Au(I)−S− staple surface motifs.[28-30] This hypothesis suggested that 18 thiol groups (cysteine residues) in a protein template were necessary to form the staple surface motifs. However, Au nanoclusters have been

synthesized using proteins with much fewer cysteine residues than that of BSA, such as insulin (6 cysteines)[26] and trypsin (7 cysteines).[24] Thus, the stabilization mechanism of Au nanoclusters in proteins remains an open question.

Apart from the nanocluster formation, the optical properties of fluorescent nanoclusters are subject to various local environmental conditions, such as pH,[31] the addition of chemicals,[32, 33] and protein absorption.[34] It remains unclear how the protein templates affect the nanocluster behaviours under various environmental conditions. Furthermore, fluorescent Au nanoclusters are normally conjugated to other molecules or immobilized onto surfaces to serve as fluorescent tags or sensing signal. However, little has been done to investigate the immobilization effects on the fluorescent properties of Au nanoclusters.

In this article, we systematically investigated the fundamental issues related to protein-Au nanoclusters by comparing 4 model protein systems (*e.g.*, bovine serum albumin-BSA, lysozyme, trypsin, and pepsin). Specifically, we studied: (1) the effects of protein size and amino acid contents on the nanocluster formation and fluorescent properties, (2) the chemical and photo stability of Au nanoclusters produced by three different proteins, and (3) the immobilization effects on Au nanoclusters generated by different proteins. We discovered that the balance of amine and tyrosine/tryptophan containing residues was critical for nanocluster formation. Protein templates with low cysteine contents caused blue shifts in the fluorescent emissions and differences in fluorescent lifetimes of the Au nanoclusters. Furthermore, the protein size served as a critical factor for the photostability and long-term stability of Au nanoclusters. The size of the protein also affected the Au nanocluster behaviour after immobilization. The fundamental understanding of protein-Au nanocluster interactions will lead to further advancement in nanocluster design and synthesis, beneficial to biological and biomedical applications.

Experiments

Chemicals. All the proteins were purchased in lyophilized-powder form and used without further purification. These proteins include: Bovine serum albumin (BSA, OmniPur), lysozyme (egg white, OmniPur), trypsin (bovine pancreas, Alfa Aesar), and pepsin (proteomic grade, Amresco). Gold chloride aqueous solution ($HAuCl_4$, 0.2 wt%) was purchased from Electron Microscopy Sciences.

Synthesis of protein-encapsulated gold nanoclusters. The fluorescent Au nanoclusters were synthesized following a procedure similar to our previously-reported method.[28] To investigate the effects of protein characteristics, four sets of experiments were performed: (1) The molar ratios of proteins to Au were kept the same, where 1 mL of freshly prepared protein solutions (BSA - 12.5 mg, trypsin - 4.6 mg, lysozyme - 2.7 mg, or pepsin - 6.5 mg) were mixed with 0.85 mL of cold $HAuCl_4$ solutions (0.2 wt%). (2) The ratios of the amine functional groups to Au were kept the same (4 to 1, where 1 mL of freshly prepared protein solutions (BSA - 12.5 mg, trypsin - 24.4 mg, and lysozyme - 15.0 mg) were mixed with 0.85 mL of cold $HAuCl_4$ solutions (0.2 wt%). (3) The molar ratios of tyrosine/tryptophan to Au were kept the same, where 1 mL of freshly prepared protein solutions (BSA - 12.5 mg, trypsin - 7.8 mg, lysozyme - 7.1 mg) were mixed with 0.85 mL of cold $HAuCl_4$ solutions (0.2 wt%). (4) The Au amount was kept the same while the amounts of proteins were adjusted to achieve the highest fluorescent intensities. Specifically, 1 mL of freshly prepared protein solutions (BSA - 12.5 mg, trypsin - 12.5 mg, or lysozyme - 15 mg) were mixed with 0.85 mL of cold $HAuCl_4$ solutions (0.2 wt%). For all the reactions, the reaction mixtures were stirred at room temperature for an hour, allowing for the complexation of Au ions with protein molecules. Then, 0.5 mL of NaOH solution (1 M) was added into each reaction mixture, which was then kept at 45 °C for desirable times depending on the protein. The obtained yellowish Au nanocluster solutions were used for characterization, stability tests, and immobilization studies. The isoelectric points (PIs) of the proteins were measured by titrating hydrochloric acid (HCl) to the solution until proteins were fully precipitated out, forming a clear solution.

Lifetime measurements. Fluorescence lifetimes of the protein-Au nanoclusters in HEPES buffer (20 mM, pH 7.4) were measured with an Edinburgh Photonics Mini-Tau time-resolved fluorometer using the time-correlated single photon counting technique (TC-SPC). The samples were excited by a diode laser emitting at 485 nm, with pulse width of 150 ps set to a 20 kHz pulse repetition rate. Control of the excitation power was achieved through a continuously variable neutral density filter wheel to collect ca. 400 photons/s (2% of excitation rate). A Thorlabs long-pass filter with a 600 nm cut-on wavelength was used for emission selection. Photons were detected over a time range up to 20 μs by a high-sensitivity photomultiplier tube. Decay curves were accumulated until 10,000 counts were collected at the highest peak in the curve. The sample temperature was controlled to 25 °C by an external circulating water bath. The intensity decay data was fitted to the following two-exponential model using a non-linear curve fitting routine implemented in house in the Mathematica v. 9.0 software.

Stability tests. The stability of the protein-encapsulated Au nanoclusters was studied by monitoring their fluorescence change under various conditions, such as pH, buffers, temperature, and UV radiation. The pH effects were studied by adjusting the pH values of the protein-encapsulated Au nanocluster solutions with HCl/NaOH in a cycle (pH= 12→9→7→5→7→9→12). At each pH, the solution was allowed equilibrating for 20 minutes before fluorescence measurement. The effects of the buffer conditions were achieved via dialysis of the nanocluster water solution in buffers for 4 hours. These buffers include phosphate buffered saline (PBS), 4-(2- hydroxyethyl)-1-piperazineethanesulfonic acid (HEPES), 2-(N-morpholino)ethanesulfonic acid (MES), and 2-amino-2-hydroxymethyl-propane-1,3-diol (Tris). The photostability was studied by measuring the fluorescence of the Au nanoclusters after UV radiation (0, 15 min, 30 min, 1, 2, or 5 hours). The temperature effects were studied by merging the nanocluster solutions in a water bath at pre-set temperatures for 20 minutes and then immediately measuring their fluorescent emission. The temperature was also set in a cycle (22→37→45→55→45→37→22 °C). The long-term stability of the nanoclusters was studied both in solution and in powder form.

Immobilization effects. The immobilization effects were studied by immobilizing the protein-encapsulated Au nanoclusters onto iron oxide nanoparticle surfaces following our previously reported procedures.[28] In brief, 12 nm spherical iron oxide nanoparticles were prepared using our modified "heat-up" method.[35-37] and then dopamine molecules were attached on the nanoparticle surfaces via a ligand exchange approach.[35] The catechol groups on the nanoparticle surfaces can effectively interact with proteins upon activation. Briefly, 1.28 mL freshly-prepared lysozyme-gold nanocluster solution was mixed with 0.5 mL activated iron oxide nanoparticle solution (1 mg/mL). After

12 hour incubation (22 °C), the conjugated nanoparticles were magnetically separated out of the solution. This process was repeated twice to remove free nanoclusters. The integrated nanostructures were then re-dispersed in water (0.5 mL) for further characterization. Alternatively, the Au nanoclusters were immobilized onto the inner surface of glass vials (2 mL) through a dopamine coating layer, and then the immobilized nanoclusters was immerged inside water to avoid drying. The glass vials with the immobilized nanoclusters were measured directly on the fluorescent spectrometer.

Characterization. The fluorescent spectra of protein-encapsulated Au nanoclusters were collected using a Cary Eclipse fluorescence spectrophotometer. The UV−visible spectra were recorded on a Shimadzu UV−visible spectrophotometer (UV-1700 series). The morphology and size of the protein-encapsulated gold nanoclusters were examined under transmission electron microscopy (TEM, FEI Tecnai, F-20, and 200 kV). The surface chemistry of the nanoparticles was studied by Fourier transform infrared spectroscopy (FTIR).

Results and Discussion

The effects of the protein sizes and amino acid contents on the formation of the fluorescent Au nanoclusters were studied using four model proteins (BSA, lysozyme, trypsin, and pepsin). During the synthesis of Au nanoclusters, several groups of amino acids are critically important to the formation and stabilization of the nanoclusters. First, the positively charged amino acids (*e.g.*, arginine and lysine) are responsible for the coordination of the $AuCl_4^-$ ions, which determine the amounts of Au can be incorporated into the proteins. Second, the amount of trypsin/tryptophan residues is important to reduce the Au ions, thus directly influencing the reaction rate. Finally, the cysteine residues are an important group to stabilize the Au nanoclusters because of the strong interaction between Au and thiol groups. Table 1 shows the characteristics of the four proteins, including protein sizes and contents of key amino acid residues. The difference in these characteristics serves as the basis for cross-comparison. The sizes of proteins decrease in the order of BSA> pepsin > trypsin > lysozyme, while except for BSA, the other three proteins have similar cysteine content (pepsin - 7, trypsin - 7, and lysozyme - 8). The considerable difference in amine-containing residues among these four proteins, such as lysine (BSA - 60, trypsin - 14, lysozyme - 6, and pepsin - 1) allows studying the role of amine groups in the nanocluster formation. The amine-containing residues are key groups to complex Au ions and subsequently determine the Au uptake.

Tab. 1 The characteristics of four model proteins

Amino acid # (to Au^{3+}) \ Proteins		BSA (66 kDa) (636 AA)	Trypsin (24 kDa) (223 AA)	Lysozyme (14 kDa) (129 AA)	Pepsin (34 kDa) (327 AA)
(a)	Arginine: Au^{3+}	26	2	11	2
	Lysine: Au^{3+}	60	14	6	1
	Histidine: Au^{3+}	16	3	1	1
	Total (positive-charged) AA to Au^{3+}	*102*	*19*	*18*	*4*
(b)	Tyrosine: Au^{3+}	21	10	3	18
	Tryptophan: Au^{3+}	3	4	6	6
	Total (reducing) AA to Au^{3+}	*24*	*14*	*9*	*24*
(c)	Cysteine: Au^{3+}	35	7	8	7

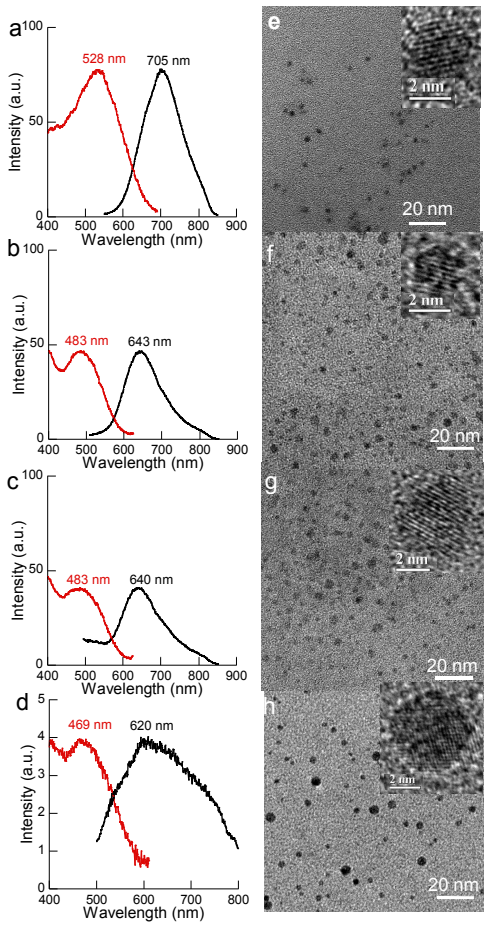

Fig. 1 Protein-encapsulated Au nanoclusters: fluorescent emission (black)/excitation (red) spectra and TEM images of Au nanoclusters generated from BSA (a and e), trypsin (b and f), lysozyme (c and g), and pepsin (d and h).

To investigate the effects of protein characteristics, four sets of experiments were performed: (1) the same molar ratio of protein to Au, (2) the same molar ratio of the amine functional groups to Au, (3) the same molar ratio of tyrosine/tryptophan to Au, and (4) excess proteins with the same amount of Au. The molar ratio of protein to Au was set at 0.04 based on previous reports that Au_{25} nanoclusters were generally produced with BSA proteins.[23] Figure 1 a-d shows the fluorescent emission and excitation spectra of the nanoclusters generated using BSA (12.5 mg/mL), trypsin (4.6 mg/mL), lysozyme (2.7 mg/mL, and pepsin (6.5 mg/mL). Compared to the emission peak ($\lambda_{em,\ max}$705 nm) of BSA-Au nanoclusters, the emission maxima of the Au nanoclusters produced using trypsin, lysozyme, and pepsin showed more than 60 nm blue shifts (e.g., trypsin - 643 nm; lysozyme - 640 nm, and pepsin - 620 nm) and with much lower fluorescent intensity, in particular for the pepsin reaction. The low fluorescent intensities were mainly due to the ineffective protection of the protein templates, leading to the formation of large size nanoparticles (Figure 1f-h). However, the typical 520 nm absorption peak of Au nanoparticles was barely detected for both trypsin and lysozyme samples (Figure S1), likely because of the percentage of the large nanoparticles was low. Interestingly, the pepsin reaction only showed detectable fluorescence after 1 h reaction, and then the fluorescence kept decreasing and was barely detectable after 4 h. Instead, the typical UV-visible absorption peak at 520 nm of Au nanoparticles was clearly

observed (Figure S2), indicating the formation of larger Au nanoparticles. The formation of Au nanoparticles rather than fluorescent nanoclusters for pepsin can be understood by the amine-containing and tyrosine/tryptophan residues in pepsin. Pepsin only contains 4 amine-containing residues, which did not allow effective complexation with $AuCl_4^-$ ions. Further, the high tyrosine/tryptophan content rapidly reduced the Au ions, leading to the formation of Au nanoparticles. This observation is inconsistent with previous reports on the formation of Au nanoclusters with pepsin.[25] We believe that the inconsistence is due to the protein source and purity, where other components might contribute to the formation of Au nanoclusters. Because of the difficult to produce pepsin-Au nanoclusters with high fluorescence intensity, the rest of comparison studies were primarily on Au nanoclusters generated using BSA, trypsin and lysozyme).

The blue shifts in fluorescent emissions of trypsin and lysozyme could be from either smaller nanoclusters or environmental effects. Based on the TEM images (Figure 1 f and g), wide size distributions of the Au nanoclusters were observed for both samples. In addition, the HRTEM did show smaller cluster sizes. We attributed the low fluorescent intensity and wide size distribution of the Au nanoclusters to the ineffective protection because of the smaller sized proteins and low cysteine contents. To ensure that enough proteins were available to protect the nanoclusters, the protein amounts of trypsin and lysozyme were adjusted to achieve the highest fluorescent intensity. After optimization, the proteins to Au ratios were found to be 0.13 to 1 for trypsin and 0.18 to 1 for lysozyme, which was much higher than that of BSA to Au (0.04 to 1). Trypsin and lysozyme have similar numbers of thiol groups; the higher amount of lysozyme required to stabilize the Au nanoclusters suggested the importance of protein size.

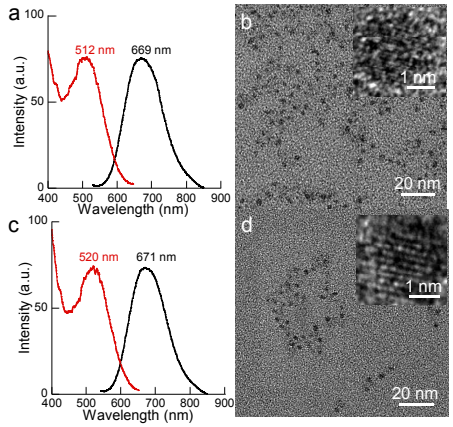

Fig.2 Fluorescent emission (black)/excitation (red) spectra and TEM images of Au nanoclusters generated from excess trypsin (a and b), and lysozyme (c and d).

Figure 2 shows the fluorescent emission/excitation plots and TEM images of Au nanoclusters generated with excess trypsin (12.5 mg/mL) and lysozyme (15 mg/mL). Compared to the emission peak ($\lambda_{em, max}$705 nm) of BSA-Au nanoclusters in Figure 1a, the emission maxima of the Au nanoclusters produced using excess trypsin and lysozyme showed more than 30 nm blue shift (e.g., trypsin - 669 nm; lysozyme - 671 nm). However, with enough proteins, uniform Au nanoclusters were produced using both trypsin and lysozyme (Figure 2b and d). Interestingly, the sizes of the Au nanoclusters from excess lysozyme and trypsin were very similar to that of the BSA-Au nanoclusters (Figure 1e).

Therefore, we believe that the blue shifts in fluorescent emissions were a result of local environments (e.g., coordinating functional groups, hydrophobicity). Previous reports on BSA-Au nanoclusters suggested that the fluorescent emission was from Au_{25} nanoclusters, including a core (Au_{13}) emission at higher wavelength and an emission from the surface staple motif [-S-Au-S-Au-S-] at lower wavelength.[29, 30] With this assumption, 18 cysteine residues are required to form six staple surface motifs. For proteins with less thiol contents, such as trypsin (7) and lysozyme (8), the formation of the surface staple motif in a single protein is limited. To stabilize the Au nanoclusters, either multiple proteins are involved or other amino acids (e.g., $-NH_2$) contribute to stabilizing the Au nanoclusters.

Here, we proposed that the amine groups were involved in the stabilization of the Au nanoclusters for proteins without enough thiol groups based on previous reports on Au surface interactions with various functional groups (thiol > amine > hydroxyl).[38, 39] Lack of cysteine residues causing blue shifts in fluorescent emissions of protein-Au nanoclusters was also observed in myoglobin (no cysteine) stabilized Au nanoclusters.[40] Thiol groups are known to form chemical bonds on Au surfaces; In contrast, amine groups are generally believed to form coordination bonds, where the lone electron pair of nitrogen involving coordination with the empty orbital of Au complex. These two types of functional groups have different ability of providing electrons and thus the surface states of Au complex. Our hypothesis of amine-involvement in nanocluster stabilization was further supported by measuring the pIs of the proteins before and after Au nanocluster encapsulation via titration. Before Au nanocluster encapsulation, the pIs of BSA, trypsin and lysozyme were experimentally determined to be 4.5, 7, and 10.5, respectively. After Au nanocluster encapsulation, the pI of BSA remained unchanged, but the pIs of trypsin and lysozyme significantly reduced to 5 and 5.5, respectively. The pI changes in lysozyme and trypsin indicated the involvement of the amine groups during the encapsulation of Au nanoclusters.

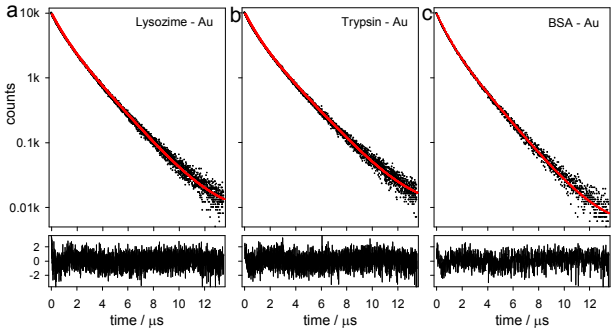

Fig. 3 Time-resolved fluorescence lifetime analysis of: (a) Lyso-Au (b) Try-Au, and (c) BSA-Au nanoclusters.

To further investigate the effects of ligands on the properties of the Au nanoclusters, the fluorescent lifetimes of all three types of Au nanoclusters were measured with an Edinburgh Photonics Mini-Tau time-resolved fluorometer using the time-correlated single photon counting technique (TC-SPC). Figure 3 shows the fluorescent emission lifetime decays and fit curves, which were fitted with multi-exponential models containing two lifetimes. The two-exponential lifetimes were 765 ns and 1976 ns for lyso-Au nanoclusters, accounting for 23.3% and 76.7% of the integrated fluorescence emission; 766 ns and 2062 ns for Try-Au nanoclusters, accounting for 24.8% and 75.2% of the integrated fluorescence emission; 711 ns and 1871 ns for BSA-Au

nanoclusters, accounting for 29.4% and 70.6% of the integrated fluorescence emission The reduced chi-square values ($\chi 2$) for each fit were: 1.12, 1.16, and 1.06, respectively.

Because multiple exponentials were necessary to fit the lifetime decays, we found it useful to present the intensity-weighted average lifetime τ_{ave} as an overall descriptor of the average time delay with which photon emission occurs after the laser pulse, which led to 1529 ns for BSA-Au, 1741 ns for trypsin-Au, and 1689 ns for lyso-Au. In all cases, the most important contribution to the emission came from the species with the longest lifetime. The study of BSA-Au nanoclusters has attributed the slow component to the triplet formation and the fast component to the trapping of surface Au(I) states.[29] The higher percentage of the fast component for BSA-Au (29.4%) than that of try-Au and lyso-Au (23.3% or 24.8%) suggested higher amount of Au(I) surface states from thiol interactions.

When the ratios of the amine functional groups to Au (4:1) were kept the same, the protein-Au nanoclusters showed similar fluorescent emission/excitation behaviours (Figure S3a) to that of the nanoclusters generated with excess proteins (Figure 2). When the amine to Au ratios were kept the same, the proteins to Au ratios turned out to be 0.04 to 1 for BSA (12.5 mg/mL) , 0.2 to 1 for both trypsin (24.4 mg/mL) and lysozyme (15 mg/mL). The ratios for trypsin and lysozyme are much higher than that of the proteins needed to stabilize Au nanoclusters, such as 0.13 to 1 for trypsin (12.5 mg/mL) and 0.18 to 1 for lysozyme (15 mg/mL). In contrast, when keeping the ratios of tyrosine/tryptophan to Au the same (1:1), the fluorescent emission/ excitation behaviours for BSA-Au nanoclusters did not change, but the fluorescent emission and excitation spectra of trypsin and lysozyme-Au nanoclusters exhibited blue shifts (Figure S3b). At the 1 to 1 reducing power to Au ratio, the proteins to Au ratios were 0.04 to1 for BSA (12.5 mg/mL), about 0.06 to 1 for trypsin (7.8 mg/mL), and 0.1 to 1 for lysozyme (7.1 mg/mL). The ratios of trypsin and lysozyme were lower than the proteins needed to stabilize Au nanoclusters, such as 0.13 to 1 for trypsin (12.5 mg/mL) and 0.18 to 1 for lysozyme (15 mg/mL).

It is expected that the encapsulation of the Au nanocluster inside the protein template interferes with the protein structure. Infrared spectroscopy offers an effective tool to study the secondary structure and the structural change of proteins.[41] In addition, the side chains of some amino acids exhibit characteristic peaks as key marker identification.[42] The FTIR spectra provide information on the secondary structural change after Au nanocluster encapsulation, because the amide bands are highly sensitive to environmental change, including amide I mainly –C=O stretching (1600-1680 cm^{-1}),[41] amide II band arising from –N-H bending (60%) and –C-N stretching (40%),[43] and amide III, the in phase combination of C-N stretching, C=O in plane bending, and C-C stretching.[44]

Compared to the IR spectra of native proteins (Figure S4), the IR spectra of the denatured proteins showed several distinct changes, such as intensity reduction of the amide I and II bands, appearance of IR bands of hydrophobic residues, and peak shifts in the amide III region. For all three proteins, the CH_2 in plane and out plane bending and rocking bands became dominant, including 1422, 991, and 877 cm^{-1} for BSA, 1429 and 880 cm^{-1} for trypsin and lysozyme. The peak shifts in the amide III regions (1129-1301 cm^{-1}) included C-N stretching and N-H bending, such as 1243 to 1278 cm-^{1} for BSA, 1236 to 1278 cm^{-1} for trypsin, and 1236 to 1305 cm^{-1} for lysozyme. Further, each protein also exhibited its specific features. For instance, BSA showed mainly hydrophobic features with the -C-H out-of plane bending at 991cm^{-1}. In addition to the exposure of hydrophobic residues, the denatured trypsin showed several typical tyrosine residues band shifts, including band 1007 cm^{-1} (phenol-OH) to 1114 cm^{-1} (phenol-O^-) after denature under basic environment along with the Tyr-O^- (-C-C- stretching) at the 1560 cm^{-1} and Try-O^- at 1496 cm^{-1} (-C-H in plane bending). Tyrosine is a very strong IR absorber, which over dominated the amide II bands. Lysozyme showed typical bands of tryptophan -C-H and –N-H bending of the indole ring at 1506 cm^{-1} and 1004 cm^{-1} along with the out plane mode of indole mode at 740 cm^{-1}.[41]

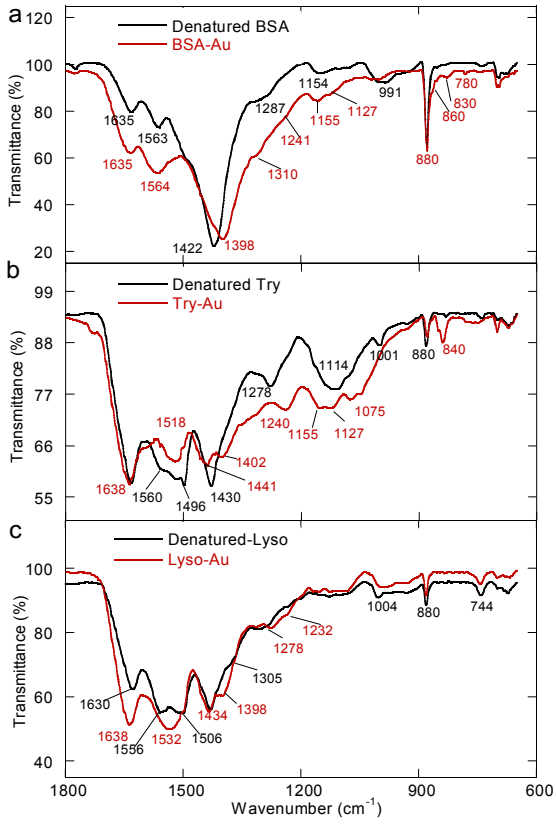

Fig. 4 FTIR spectra of protein-encapsulated Au nanoclusters and its corresponding free proteins under denatured conditions: (a) BSA, (b) trypsin, and (c) lysozyme.

Figure 4 shows the IR spectra of denatured proteins and protein-Au nanoclusters. After Au nanocluster encapsulation, all three proteins refolded to some extend with enhanced signals of the amide I and amide II bands. The shifts observed in amide III region shifted back to native states, such as 1287 to 1241 and 1310 cm^{-1} for BSA, 1278 to 1240 cm^{-1} for trypsin, and 1305 to 1278 cm^{-1} for lysozyme. The refold of BSA was also supported by the disappearance of –CH out of plane bending band (991 cm^{-1}). The $–CH_2$ bending band at 1442 cm^{-1} became a shoulder of the major 1398 cm^{-1} band (Figure 4a). In addition to the change in the hydrophobic residues, several IR bands related to -COO^- groups appeared, including the asymmetric/symmetric stretching vibration of -COO^- groups at 1564 cm^{-1} (overlapped with the amide II band) and 1398 cm^{-1}, -COO^- scissoring and rocking at 860 cm^{-1} and 830 cm^{-1},[45, 46] and -C=O out of plane bending at 780 cm^{-1}.[47] The spectra change can be easily understood by the large amount of negatively charged residues (99) in BSA and these carboxylic groups were entirely ionized at the reaction pH 12. In

contrast, trypsin protein only has 9 negatively charged residues. Compared to the free protein, the IR spectrum changes suggested the negatively charged residues were either highly exposed or close to the Au nanocluster, which enhanced the IR signal.

After Au nanocluster encapsulation, the amide I band (1638 cm^{-1}) of trypsin showed little variation, but the Tyr-O^- bands at the 1560 cm^{-1} and 1496 cm^{-1} became the characteristic tyrosine band at 1518 cm^{-1} (Figure 4b).[41] Interestingly, the side chain bands of tyrosine residues showed a significant band at 840 cm^{-1}, a key marker of tyrosine-tyrosine crosslinker,[48] which is a result of Au ion and tyrosine reduction/oxidation. The amide I and II bands of lysozyme were much enhanced (Figure 4c) after Au nanocluster encapsulation. However, no other significant changes were observed except for the disappearance of indole ring band at 1506 cm^{-1}, and the appearance of a shoulder band at 1398 cm^{-1}.

The stability of fluorescence is a key parameter to the application of Au nanoclusters as tag molecules for sensing, imaging, or detection. The stabilities of the Au nanoclusters (generated from various proteins) were systematically studied in terms of pH effects, buffer environments, photo, thermal, and long-term stability. The chemical, physical, and long-term stabilities of the protein-Au nanoclusters were studied using the nanoclusters produced with excess proteins because of the high fluorescent intensity and enough materials from the same batch for stability studies.

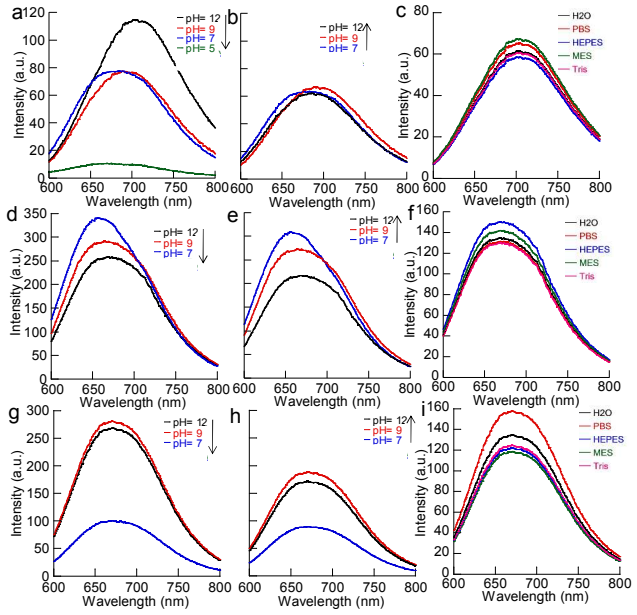

Fig. 5 pH and buffer condition effects on the fluorescent emission of Au nanoclusters generated by: (a-c) BSA, (d-f) trypsin, and (g-i) lysozyme.

All of the Au nanoclusters were produced under highly basic conditions (pH 12); however, these nanoclusters are generally utilized in physiological conditions. The pH effects were studied by monitoring the fluorescent emissions of the protein-Au nanoclusters at different pH values (12→9→7→5→7→9→12). At each pH value, the solution was equilibrated for 20 minutes before measuring. Figure 5 shows the pH effects on the fluorescent emissions of the protein encapsulated Au nanoclusters. For BSA-Au nanoclusters (Figure 5a and b), we observed an approximately 30% reduction in fluorescent intensity and a 15 nm blue shift of the $\lambda_{em,\ max}$ from pH 12 to 9. The emission intensity at pH 7 was similar to that at pH 9, but the $\lambda_{em,\ max}$ blue shifted another 10 nm. By pH 5, most of the proteins were precipitated out of the solution because of the pI of the protein and a very low fluorescent signal was detected. The lost fluorescence intensity was recovered after adjusting the pH of the solution (Figure 5b). However, the fluorescence intensities were slightly lower because of the dilution during the pH adjustment with HCl and NaOH solutions and the difficulty in re-dissolving the protein precipitates entirely. This pH dependent behaviour of the BSA-Au nanoclusters was related to the structural conformation of BSA protein. BSA remains its native conformation in a pH range of 5 - 7.5; but it changes into the basic form above pH 8. Continuous pH increase to 12 causes the completely unfold of domain I and III.[53]

For trypsin-Au nanoclusters (Figure 5d and e), the highest fluorescent intensity was observed at pH 7 because trypsin has a well ordered conformation between pH 7 and 8, but becomes considerably less ordered at more acidic and more basic pH values.[54] After going through the pI of the protein, the fluorescent intensities were slightly lower due to dilution of the solution and the difficulty in re-dispersing the aggregates entirely. Compared to the ~ 25 nm blue shift of the $\lambda_{em,\ max}$ from pH 12 to 7 for BSA-Au nanoclusters, the fluorescent emission of trypsin-Au nanoclusters exhibited ~10 nm blue shift from pH 12 to7. At pH 5, the protein-Au nanoclusters were precipitated out and no fluorescent spectrum was collected. For lysozyme-Au nanoclusters (Figure 5g and h), the $\lambda_{em,\ max}$ did not shift with pH likely due to the high stability of lysozyme in a wide pH range. The decrease in intensity was mainly due to the precipitation of the lysozyme-Au nanoclusters.

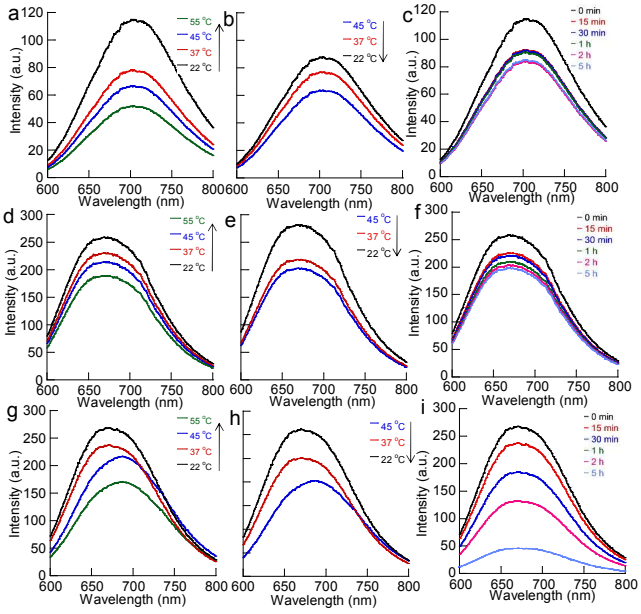

Fig. 6 Temperature and UV-radiation effects on the fluorescent emissions of the Au nanoclusters generated by: (a-c) BSA, (d-f) trypsin, and (g-i) lysozyme.

For biological applications, fluorescent nanoclusters are generally applied in biological buffers; therefore, the stabilities of the Au fluorescent nanoclusters were studied in various buffers, including PBS, MES, Tris, and HEPES. Figure 5c, f, and i shows the florescent emission plots at various conditions. Compared to emissions of the Au nanoclusters in water at pH 7, dialysis with biological buffers at pH 7 did not affect the fluorescence emission much. However, we did observe a slight intensity variation

among these three types of Au nanoclusters. For example, the highest intensities were observed in MES for BSA-Au nanoclusters, HEPES for trypsin-Au nanoclusters and PBS for lysozyme-Au nanoclusters.

Generally, during applications, a laser is applied to excite the nanoclusters. Depending on the duration, the laser can heat up and/or photobleach the tag molecules. The temperature effects on the protein-Au nanoclusters were studied in a cycle (22→37→45→55→45→37→22 °C) by merging the nanocluster solutions in a water bath at pre-set temperatures. After 20 minute equilibration, the nanocluster solutions were immediately measured. Figure 6 shows the fluorescent emission plots of the protein-Au nanoclusters at different temperatures. For all of the three types of Au nanoclusters, the fluorescence intensities decreased as the temperature increased, mainly due to the increased photo collision at higher temperatures. However, the fluorescence was largely recovered once the nanocluster solutions were at lower temperature. In addition to the decrease in fluorescent intensity, the lysozyme-Au nanoclusters also showed an approximately 20 nm red shift likely because of aggregation. However, this aggregation process was reversible, similar to the pH effects.

The photostability (i.e. the decrease in fluorescent intensity upon light irradiation) of a fluorescent tag determines the duration of a measurement or test. The photostability of the protein-Au nanoclusters were studied under UV light radiation (365 nm, 6 W/cm^2) in water at pH 12 (Figure 6 c, f and i). The fluorescence intensity of BSA-Au nanoclusters dropped 20% at the first 15 minutes. Then, the Au nanoclusters showed great photo stability with only ~ 5% loss after 5 hour radiation (Figure 6c). The great UV stability of BSA-Au nanoclusters can be understood by the large size of the protein template (636 aa) and the formation of the complete surface staple motifs with the involvement of 18 thiol groups. Similar to the BSA-Au nanoclusters, the trypsin-Au nanoclusters exhibited 25% fluorescence drop after 5 h with a quick loss of 15% at the first 15 minutes (Figure 6f). Compared to BSA, trypsin has a much smaller size (223 aa) and fewer thiol groups (7) without the formation of a complete coverage of surface staple motifs. The fluorescent intensity of lysozyme-Au nanoclusters dropped approximately 60% after 1 h and 80% after 5 hours. The lysozyme has similar thiol content to trypsin, but with a much smaller size (129 aa) (Figure 6i). Therefore, we concluded that protein size was the main factor contributing to the photostability of the protein-encapsulated nanoclusters, not the $-S-Au(I)-S-Au(I)-S-$ staple surface motifs.

The long-term stability of the Au nanoclusters was studied in powder and solution form for each protein. The Au nanoclusters generated from all three proteins showed higher stability in powder form than that in solution (Figure S5). For example, at 4 °C, the BSA-Au nanoclusters stored in powder form retained 96% of the fluorescent intensity after one year, while the fluorescence intensity of the same sample in solution reduced to 75% after one month. Similar trends were observed for the trypsin-Au nanoclusters (92% in powder and 80% in solution) and lysozyme-Au nanoclusters (90% in powder and 75% in solution) after one month. Except for the fluorescent intensity, the $\lambda_{em,\ max}$ of BSA-Au nanoclusters showed no shift. In contrast, trypsin-Au nanoclusters showed no change in powder form, but with a red shift in $\lambda_{em,\ max}$ in solution, an indication of aggregation. The aggregation in solution was likely because the proteins were subject to protease in solution. The lysozyme-Au nanoclusters showed red shifts in both powder and solution form. This observation suggested that the protein size is a key parameter for long-term stability.

To understand the immobilization effect, protein-encapsulated Au nanoclusters were covalently conjugated onto iron oxide nanoparticle surfaces using our previously reported procedure (Figure 7).[28] Because of the extremely small sizes of the Au nanoclusters, they were barely seen on the iron oxide nanoparticles. However, small darker spots on the nanoparticle surfaces could be observed via carefully examination. After immobilization, the $\lambda_{em,\ max}$ of the BSA-Au nanoclusters blue shifted about 25 nm and maximum excitation blue shifted about10 nm. The blue shifts were likely resulted from the conformational change of BSA protein, which altered the local environment of the Au nanoclusters. BSA is known to have several dynamic conformations. After immobilization on the nanoparticle surfaces, the dynamic conformation of BSA was significantly reduced. In contrast to the BSA-Au nanoclusters, both trypsin-Au and lysozyme-Au nanoclusters showed much broader fluorescent emission and excitation peaks after immobilization. The fluorescent emission peaks were blue shifted while the fluorescent excitation peaks were red shifted. We attributed these changes to the involvement of iron oxide nanoparticles during excitation and emission, because iron oxide nanoparticles have strong absorption in the visible range. This effect could only take place when the nanoclusters were close to the surface of iron oxide nanoparticles. The size of BSA protein is much larger than that of trypsin and lysozyme, and showed only minimal effects from the iron oxide nanoparticles.

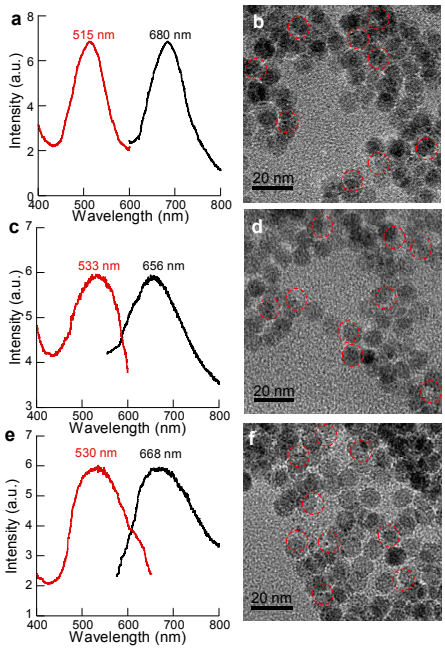

Fig. 7 Protein-Au nanoclusters immobilized on iron oxide nanoparticle surface: fluorescent emission/excitation plots and TEM images of BSA (a and b), trypsin (c and d), and lysozyme (e and f).

To verify our hypothesis, we conducted experiments by simply mixing the Au nanocluster solutions with iron oxide nanoparticles and then measured the fluorescent emission and excitation before and after the addition of iron oxide nanoparticles. Figure S6 showed the fluorescent excitation/emission plots of protein-Au nanoclusters before and after the addition of iron oxide nanoparticles. For all these samples, significant intensity decrease

was observed due to the strong absorption of iron oxide nanoparticles in visible range, but the emission peak (λ_{em}, max) was not affected. In contrast, the excitation peak red shifted. This observation was mainly because the iron oxide nanoparticles have absorption in the visible range, which interfered with the excitation but not the emission. Compare the spectra of the simply mixed and the immobilized nanocluster samples, the immobilization effects on the Au nanoclusters can be clearly identified.

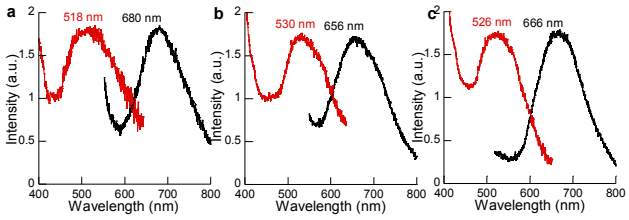

Fig. 8 The fluorescent emission/excitation plots of protein-Au nanoclusters immobilized on the inner surface of glass vials: (a) BSA, (b) trypsin, and (c) lysozyme.

Alternatively, the protein-Au nanoclusters were immobilized on the inner surface of glass vials. Figure 8 shows the fluorescent emission/excitation plots of the immobilized Au nanoclusters immerged in water. Similar emission and excitation shifts were observed for both immobilizations experiments. Therefore, we believe that the protein dynamic conformation was primarily responsible for changes in the fluorescence.

Conclusions

In summary, the effects of protein size and amino acid content on the protein-encapsulated Au nanoclusters were studied systematically. The experimental results suggested that a balance of the amine-containing and tyrosine/tryptophan residues was critical for the formation and stabilization of the Au nanoclusters. For example, pepsin with a few amine-containing residues but much higher amount of tyrosine/tryptophan was not able to produce Au nanoclusters, leading to the formation of larger size Au nanoparticles. In addition, the cysteine content is critical to form surface staple residue and fluorescent emission. Lower cysteine content (< 18 per protein) caused blue shifts of the emission spectra and difference in fluorescent lifetimes due to the possible contribution from amine-containing residues in the stabilization of the Au nanoclusters. Furthermore, the size of the protein template was found to be critical to the photo, thermal, and chemical stability of the Au nanoclusters. Finally, regardless of the size of the protein, immobilization effects were observed for all three types of Au nanoclusters.

Acknowledgments

This work is supported by NSF-DMR 0907204 and DMR1149931. We acknowledge the UA Central Analytical Facility (CAF) and the Biological Science Department for the use of TEM. We also acknowledge the highly useful discussion with Professor Jin Zhang (University of California-Santa Cruz).

Notes and references

[a] *Department of Chemical and Biological Engineering, The University of Alabama, Tuscaloosa, AL35487, USA. Corresponding authors: (Y.B.)ybao@eng.ua.edu Tel: 01-205-348-9869; Fax: 01-205-348-7558*

[b] *Alabama Innovation and Mentoring of Entrepreneurs, The University of Alabama, Tuscaloosa, AL35487, USA.*

[c] *Department of Chemistry, The University of Alabama, Tuscaloosa, AL35487, USA.*

1. N. Makarava, A. Parfenov and I. V. Baskakov, *Biophys. J.*, 2005, **89**, 572-580.
2. R. C. Triulzi, M. Micic, S. Giordani, M. Serry, W. A. Chiou and R. M. Leblanc, *Chem. Commun.*, 2006, **48**, 5068-5070.
3. J. M. Slocik, J. T. Moore and D. W. Wright, *Nano Lett.*, 2002, **2**, 169-173.
4. J. Zheng, P. R. Nicovich and R. M. Dickson, *Annu. Rev. Phys. Chem.*, 2007, **58**, 409-431.
5. S. Link, A. Beeby, S. FitzGerald, M. A. El-Sayed, T. G. Schaaff and R. L. Whetten, *J. Phys. Chem. B*, 2002, **106**, 3410-3415.
6. T. P. Bigioni, R. L. Whetten and O. Dag, *J. Phys. Chem. B*, 2000, **104**, 6983-6986.
7. O. Varnavski, R. G. Ispasoiu, L. Balogh, D. Tomalia and T. Goodson, *J. Chem. Phys.*, 2001, **114**, 1962-1965.
8. Y. Bao, C. Zhong, D. M. Vu, J. P. Temirov, R. B. Dyer and J. S. Martinez, *J. Phys. Chem. C*, 2007, **111**, 12194-12198.
9. Y. Negishi and T. Tsukuda, *Chem. Phys. Lett.*, 2004, **383**, 161-165.
10. Y. Bao, H. C. Yeh, C. Zhong, S. A. Ivanov, J. K. Sharma, M. L. Neidig, D. M. Vu, A. P. Shreve, R. B. Dyer, J. H. Werner and J. S. Martinez, *J. Phys. Chem. C*, 2010, **114**, 15879-15882.
11. W. An, L. Wintzinger, C. H. Turner and Y. Bao, *Nano-Life*, 2010, **1**, 133-143.
12. G. Liu, Y. Shao, F. Wu, S. Xu, J. Peng and L. Liu, *Nanotechnol.*, 2013, **24**, 015503.
13. G. Liu, Y. Shao, K. Ma, Q. Cui, F. Wu and S. Xu, *Gold Bull.*, 2012, **45**, 69-74.
14. T. A. C. Kennedy, J. L. MacLean and J. Liu, *Chem. Comm.*, 2012, **48**, 6845-6847.
15. D. M. Chevrier, A. Chatt and P. Zhang, *J. Nanophoton*, 2012, **6**, 064504(13).
16. J. Xie, Y. Zheng and J. Ying, *J. Am. Chem. Soc.*, 2009, **131**, 888-889.
17. X. L. Guevel, B. Hotzer, G. Jung, K. Hollemeyer, V. Trouillet and M. Schneider, *J. Phys. Chem. C*, 2011, **115**, 10955-10963.
18. Y. Yue, T. Liu, H. Li, Z. Liu and Y. Wu, *Nanoscale*, 2012, **4**, 2251-2254.
19. H. Wei, Z. Wang, L. Yang, S. Tian, C. Hou and Y. Lu, *Analyst*, 2010, **135**, 1406-1410.
20. T. Chen and W. Tseng, *Small*, 2012, **8**, 1912-1919.
21. X. L. Guevel, N. Daum and M. Schneider, *Nanotechnol.*, 2011, **22**, 275103.
22. P. L. Xavier, K. Chaudhari, P. K. Verma, S. K. Pal and T. Pradeep, *Nanoscale*, 2010, **2**, 2769-2776.
23. K. Chaudhari, P. L. Xavier and T. Pradeep, *ACS Nano*, 2011, **5**, 8816-8827.
24. H. Kawasaki, K. Yoshimura, K. Hamaguchi and R. Arakawa, *Anal. Sci.*, 2011, **27**, 591-596.
25. H. Kawasaki, K. Hamaguchi, I. Osaka and R. Arakawa, *Adv. Funct. Mater.*, 2011, **21**, 3508-3515.
26. C. Liu, H. Wu, Y. Hsiao, C. Lai, C. Shih, Y. Peng, K. Tang, H. Chang, Y. Chien, J. Hsiao, J. Cheng and P. Chou, *Angew. Chem. Int. Ed.*, 2011, **50**, 7056-7060.
27. F. Wen, Y. Dong, L. Feng, S. Wang, S. Zhang and X. Zhang, *Anal. Chem.*, 2011, **83**, 1193-1196.
28. Y. Xu, S. Palchoudhury, Y. Qin, T. Macher and Y. Bao, *Langmuir*, 2012, **28**, 8767-8772.
29. X. Wen, P. Yu, Y. R. Toh, A. C. Hsu, Y. C. Lee and J. Tang, *J. Phys. Chem. C*, 2012, **116**, 19032-19038.
30. X. Wen, P. Yu, Y. R. Toh, A. C. Hsu, Y. C. Lee and J. Tang, *J. Phys. Chem. C*, 2012, **116**, 11830-11836.
31. X. Cao, H. Li, Y. Yue and Y. Wu, *Vib. Spectrosc.*, 2013, **65**, 186-192.
32. D. Xiang, G. Zeng, K. Zhai, L. Li and Z. He, *Anal.*, 2011, **136**, 2837-2844.
33. Z. Luo, X. Yuan, Y. Yu, Q. Zhang, D. T. Leong, J. Y. Lee and J. Xie, *J. Am. Chem. Soc.*, 2012, **134**, 16662-16670.

34. L. Shang, S. Brandholt, F. Stockmar, V. Trouillet, M. Bruns and G. U. Nienhaus, *Small*, 2012, **8**, 661-665.
35. Y. Xu, Y. Qin, S. Palchoudhury and Y. Bao, *Langmuir*, 2011, **27**, 8990-8997.
36. S. Palchoudhury, Y. Xu, J. Goodwin and Y. Bao, *J. Mater. Chem.*, 2011, **21**, 3966-3970.
37. S. Palchoudhury, Y. Xu, J. Goodwin and Y. Bao, *J. Appl. Phys.*, 2011, **109**, 07E314.
38. X. Zhu, Q. Yang, J. Huang, I. Suzuki and G. Li, *J. Nanosci. Nanotechnol*., 2008, **8**, 353-357.
39. L. Polavarapu and Q. Xu, *Nanotechnol*., 2008, **19**, 075601.
40. S. Volden, S. M. Lystvet, O. Halskau and W. R. Glomm, *RSC Adv.*, 2012, **2**, 11704-11711.
41. A. Barth, *Biochim. Biophys. Acta-Bioenerg.*, 2007, **1767**, 1073-1101.
42. A. Barth, *Prog. Biophys. Mol. Bio.*, 2000, **74**, 141-173.
43. M. Jackson and H. H. Mantsch, *Crit. Rev. Biochem. Mol. Biol*., 1995, **30**, 95-120.
44. G. Anderle and R. Mendelsohn, *Biophys. J*., 1987, **52**, 69-74.
45. I. Rehman, Z. Movasaghi and S. Rehman, *Vibrational Spectroscopy for Tissue Analysis*. Taylor & Francis, 1st edn., 2013.
46. J. T. L. Navarrete, V. Hernandez and F. J. Ramirez, *J. Mol. Struct*., 1995, **348**, 249-252.
47. M. E. Rudbeck, S. Kumar, M. A. Mroginski, S. O. N. Lill, M. R. A. Blomberg and A. Barth, *J. Phys. Chem. A*, 2009, **113**, 2935-2942.
48. K. D. Anderson, J. M. Slocik, M. E. McConney, J. O. Enlow, R. Jakubiak, T. J. Bunning, R. R. Naik and V. V. Tsukruk, *Small*, 2009, **5**, 741-749.
49. B. B. Koleva, *Bulg. Chem. Commun.*, 2008, **40**, 456-463.
50. B. B. Ivanova, *Spectrochim. Acta A-Mol. Biomol. Spectrosc.*, 2006, **64**, 931-938.
51. R. Sanghi and P. Verma, *Adv. Mater. Lett.*, 2011, **2**, 193-199.
52. M. Bouchard and M. Auger, *Biophys. J.*, 1993, **65**, 2484-2492.
53. B. Ahmad, M. Z. Kamal and R. H. Khan, *Protein Pept. Lett*., 2004, **11**, 307-315.
54. M. L. Simon, K. László, M. Kotormán and B. A. Szajáni, *Acta Biol. Szeged.*, 2001, **45**, 43-49.

A table of contents entry

The size and composition of the protein templates are critically important to the formation, fluorescence, and stability of Au nanoclusters